# Formation of Triniobocene Cationic and Neutral Mononiobocene Species as a Function of Solvent in the Reaction of $Cp_2Nb\{(\mu\text{-}H)_2BR_2\}$ ($R_2 = C_4H_8$, $C_5H_{10}$, $C_8H_{14}$) with $B(C_6F_5)_3$

Shengming Liu, Fu-Chen Liu, Gordon Renkes, and Sheldon G. Shore*

*Department of Chemistry, The Ohio State University, 100 West 18th Avenue, Columbus, Ohio 43210*

*Received August 23, 2001*

Reactions of the niobocene cyclic organohydroborates $Cp_2Nb\{(\mu\text{-}H)_2BR_2\}$ ($R_2 = C_4H_8$, $C_5H_{10}$, $C_8H_{14}$), with $B(C_6F_5)_3$ in the poorly coordinating solvent toluene and in the coordinating solvent diethyl ether give different products. In toluene, the salt $[Cp_2Nb(\mu\text{-}H)(\eta^5\text{-}\eta^1\text{-}C_5H_4)\text{-}Nb(\eta^5\text{-}\eta^1\text{-}C_5H_4)_2Nb\{(\mu\text{-}H)(\eta^5\text{-}C_5H_4B(C_6F_5)_2)\}]^+[HB(C_6F_5)_3]^-$, **1**, which contains a triniobocene cation, is formed. On the other hand in diethyl ether, the reaction of $Cp_2Nb\{(\mu\text{-}H)_2BR_2\}$ with $B(C_6F_5)_3$ produces the covalent complex $CpNb(C_6F_5)\{(\mu\text{-}H)(\eta^5\text{-}C_5H_4B(C_6F_5)_2)\}$, **2**. In the formation of these compounds $Nb^{III}$ is oxidized to $Nb^{IV}$. Upon the basis of ESR spectra, **1** and **2** are paramagnetic, each with one unpaired electron. The structures of **1** and **2** were determined by single-crystal X-ray analysis. Complex **2** forms weak adducts in the solvents THF and pyridine. The Nb−H−B bridge is cleaved at the Nb−H site to form $CpNb(C_6F_5)\text{-}(L)\{\eta^5\text{-}C_5H_4B(H)(C_6F_5)_2\}$ (L = THF, pyridine). In pyridine, a second adduct in much smaller yield is also formed, $CpNb(C_6F_5)(H)\{\eta^5\text{-}C_5H_4B(Py)(C_6F_5)_2$, with the Nb−H−B bridge being cleaved at the H−B site.



## Introduction

The compound $B(C_6F_5)_3$ and variations of this molecule have been the reagents of choice in the removal of carbanions from group IV metallocene derivatives.[1,2] One of the main goals has been the preparation of cations that might have useful properties in catalytic olefin polymerization.[1,3−5] However, there has been significantly less effort with respect to the investigation of the basic chemistry of hydride ion abstraction from metallocene derivatives. Previous studies of hydride abstraction that have been reported involve removal of a terminal hydride from the metal.[3,6,7] We found that $B(C_6F_5)_3$ abstracts a hydride ion from the zirconocene cyclic organohydroborate derivative $Cp_2ZrH\{(\mu\text{-}H)_2\text{-}BC_4H_8\}$.[6] In the poorly coordinating solvent benzene, the $[HB(C_6F_5)_3]^-$ salt of the unsupported hydrogen-bridged cation $[(\mu\text{-}H)\{Cp_2Zr(\mu\text{-}H)_2BC_4H_8\}_2]^+$ (Scheme 1, **a**) is produced. On the other hand, in the coordinating solvent $Et_2O$, the $[HB(C_6F_5)_3]^-$ salt of the $[Cp_2Zr(OEt)(OEt_2)]^+$ cation was produced (Scheme 1, **b**). Both of these reactions appear to involve initial removal of a terminal hydrogen from the zirconium atom.

**Scheme 1**

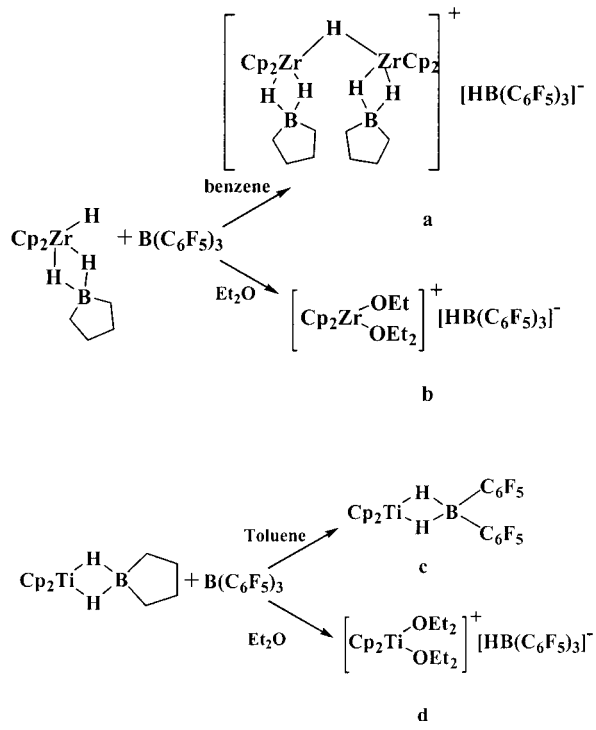


More recently we examined hydride ion abstractions[8] from the titanocene organohydroborates $Cp_2Ti\{(\mu\text{-}H)_2BR_2\}$ ($R_2 = C_4H_8$, $C_5H_{10}$, $C_8H_{14}$)[9] (Chart 1), which

(1) Chen, E. Y.-X.; Marks, T. J. *Chem. Rev.* **2000**, *100*, 1391, and references therein.
(2) Chen, E. Y.-X.; Abboud, K. A. *Organometallics* **2000**, *19*, 5541.
(3) Yang, X.; Stern, C. L.; Marks, T. J. *J. Am. Chem. Soc.* **1994**, *116*, 10015.
(4) Guram, A. S.; Jordan, R. F. In *Comprehensive Organometallic Chemistry, II*; Abel, E. W., Stone, F. G. A., Wilkinson, G., Eds.; Elsevier Science, Ltd.: New York, 1995; Vol. 4, Chapter 12.
(5) Recent reviews of cationic metallocenes and olefin polymerization: (a) A thematic issue on cationic metallecenes and homogeneous olefin polymerization: *Chem. Rev.* **2000**, *100*. (b) Abbenhuis, H. C. L. *Angew. Chem., Int. Ed.* **1999**, *38*, 1058. (c) Mcknibht, A. L.; Waymouth, R. M. *Chem. Rev.* **1998**, *98*, 2587. (d) Kaminsky, W. *J. Chem. Soc., Dalton Trans.* **1998**, 1413. (e) Bochmann, M. *J. Chem. Soc., Dalton Trans.* **1996**, 255.
(6) Liu, F.-C.; Liu, J.; Meyers, E. A.; Shore, S. G. *J. Am. Chem. Soc.* **2000**, *122*, 6106.
(7) Antinolo, A.; Carillo-Hermosilla, F.; Fernandez-Baeza, J.; Garcia-Yuste, S.; Otero, A.; Sanchez-Prada, J.; Villasenor, E. *J. Organomet. Chem.* **2000**, *609*, 123.

10.1021/om0107744 CCC: $20.00 
Publication on Web 11/21/2001

**Chart 1**

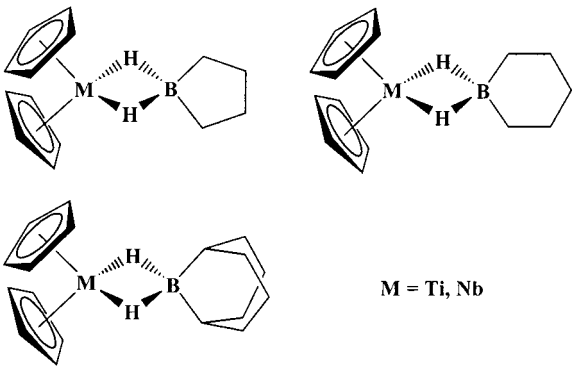


do not possess a terminal hydride−metal bond. These reactions with $B(C_6F_5)_3$ also give products that are dependent upon the type of solvent employed (Scheme 1, **c** and **d**). In a poorly coordinating solvent, the covalent metathesis product $Cp_2Ti\{(\mu\text{-}H)_2B(C_6F_5)_2\}$ was generated while the $[HB(C_6F_5)_3]^-$ salt of the titanocene cation, $[Cp_2Ti(OEt_2)_2]^+$, was isolated from the coordinating solvent diethyl ether. There is no change in the oxidation state of titanium in these reactions.

The present study is concerned with the examination of reactions of niobocene cyclic organohydroborates $Cp_2Nb\{(\mu\text{-}H)_2BR_2\}$ ($R_2$ = $C_4H_8$, $C_5H_{10}$, $C_8H_{14}$) with $B(C_6F_5)_3$ in poorly coordinating and in coordinating solvents. These niobocene complexes are comparable to the titanocene systems[9] in structure and in oxidation state (III) of the metal. As reported here, although solvent dependence was observed, remarkably different results were obtained for the group V niobocene complexes than for those produced by comparable reactions of group IV titanocene derivatives.[8]

## Results

**Formation of $[Cp_2Nb(\mu\text{-}H)(\eta^5\text{-}\eta^1\text{-}C_5H_4)Nb(\eta^5\text{-}\eta^1\text{-}C_5H_4)_2Nb\{(\mu\text{-}H)(\eta^5\text{-}C_5H_4B(C_6F_5)_2)\}]^+[HB(C_6F_5)_3]^-$, 1, in the Poorly Coordinating Solvent Toluene.** The niobocene cyclic organohydroborates $Cp_2Nb\{(\mu\text{-}H)_2BR_2\}$ ($R_2 = C_4H_8$, $C_5H_{10}$, $C_8H_{14}$) (Chart 1) react with $B(C_6F_5)_3$ in the poorly coordinating solvent toluene to produce the brown-colored salt $[Cp_2Nb(\mu\text{-}H)(\eta^5\text{-}\eta^1\text{-}C_5H_4)Nb(\eta^5\text{-}\eta^1\text{-}C_5H_4)_2Nb\{(\mu\text{-}H)(\eta^5\text{-}C_5H_4B(C_6F_5)_2)\}]^+[HB(C_6F_5)_3]^-$, **1**, as shown in reaction 1.

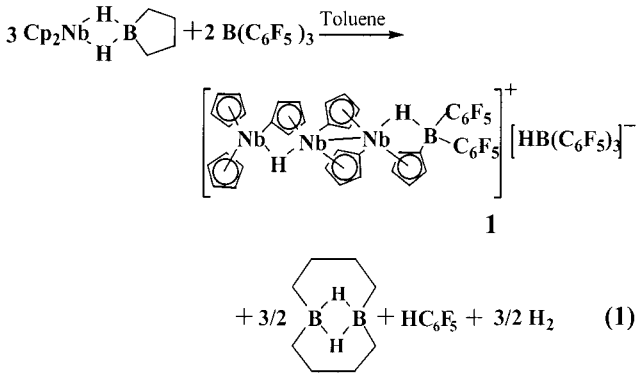


(8) Plečnik, C. E.; Liu, F.-C.; Liu, S.; Liu, J.; Meyers, E. A.; Shore, S. G. *Organometallics* **2001**, *20*, 3599.

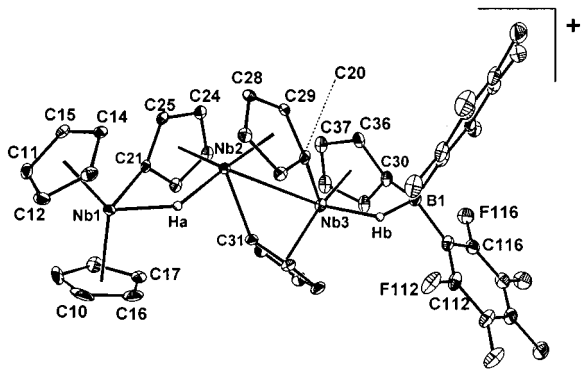


**Figure 1.** Molecular structure of the cation in $[Cp_2Nb(\mu\text{-}H)(\eta^5\text{-}\eta^1\text{-}C_5H_4)Nb(\eta^5\text{-}\eta^1\text{-}C_5H_4)_2Nb\{(\mu\text{-}H)(\eta^5\text{-}C_5H_4B(C_6F_5)_2)\}]^+[HB(C_6F_5)_3]^-$, **1**.

This compound contains the first example of a triniobocene cation. The salt is soluble in $CH_2Cl_2$, THF, and pyridine. It is slightly soluble in diethyl ether and in toluene. There is no apparent reaction with any of these solvents. Complex **1** is stable in the absence of air. Interestingly, in reaction **1** hydrogen is evolved and the niobiums are oxidized from the III oxidation state to the IV oxidation state. Pentafluorobenzene, $HC_6F_5$, is also formed (identified by GC−MS(EI): calcd for $HC_6F_5$, $m/z$ = 168.1; obsd, $m/z$ = 168.1). One other product of this reaction is also formed which is confirmed by $^{11}B$ NMR. It depends on the cyclic organohydroborate ligand employed. The transannular hydrogen-bridged 10-membered cyclic organodiborane $B_2(\mu\text{-}H)_2(\mu\text{-}C_4H_8)_2$[10] is formed when $R_2 = C_4H_8$ (reaction 1), and the organodiboranes $(\mu\text{-}H)_2(BC_5H_{10})_2$[10] and $(\mu\text{-}H)_2(BC_8H_{14})_2$[10] are formed when $R_2 = C_5H_{10}$ and $C_8H_{14}$, respectively. Yields of **1** fall in the range 45−50%.

The structure of **1** was determined by single-crystal X-ray analysis. The structure of the cation $[Cp_2Nb(\mu\text{-}H)(\eta^5\text{-}\eta^1\text{-}C_5H_4)Nb(\eta^5\text{-}\eta^1\text{-}C_5H_4)_2Nb\{(\mu\text{-}H)(\eta^5\text{-}C_5H_4B(C_6F_5)_2)\}]^+$ is shown in Figure 1. Crystal data are listed in Table 1, and selected bond lengths and bond angles are listed in Table 2.

There are two types of hydrogen bridge bonds, Nb1−Ha−Nb2 and Nb3−Hb−B1 in the cation. The Nb−H distances, Nb1−Ha (1.86(9) Å), Nb2−Ha (2.06(9) Å), and Nb3−Hb (1.94(6) Å), in the cation are not much different from those in the starting materials, $Cp_2Nb\{(\mu\text{-}H)_2BR_2\}$ ($R_2 = C_4H_8$, 1.82(3) and 1.76(3) Å; R = $C_5H_{10}$, 1.85(3) Å, R = $C_8H_{14}$, 1.80−1.89 Å).[9,11] The B−H distance (B1−Hb, 1.32(7) Å) is also close to those in the starting materials. The cation contains a covalent bond between Nb2 and Nb3, through spin pairing of the valence electron on each of these $Nb^{IV}$ atoms. This Nb2−Nb3 distance, 3.1208(8) Å, is comparable to the distance, 3.105(6) Å, between the $Nb^{IV}$ atoms in the covalent bond of the diamagnetic molecule $[(\eta^5\text{-}C_5H_5)(\eta^5\text{-}\eta^1\text{-}C_5H_4)NbH]_2$ (Figure 2a) reported by Guggenberger and Tebbe.[12] With the exception of the

(9) Liu, F.-C.; Plečnik, C. E.; Liu, S.; Liu, J.; Meyers, E. A.; Shore, S. G. *J. Organomet. Chem.* **2001**, *627*, 109.

(10) (a) Young, D. E.; Shore, S. G. *J. Am. Chem. Soc.* **1969**, *91*, 3497. (b) Köster, R. *Angew. Chem.* **1960**, *72*, 626. (c) Brown, H. C.; Negishil, E.-I. *J. Organomet. Chem.* **1971**, *26*, C67. (d) Brown, H. C.; Pai, G. G. *Heterocycles* **1982**, *17*, 77.

(11) Hartwig, J. F.; De Gala, S. R. *J. Am. Chem. Soc.* **1994**, *116*, 3661.

**Table 1. Crystallogphic Data for $Cp_2Nb(\mu\text{-}H)(\eta^5\text{-}\eta^1\text{-}C_5H_4)Nb(\eta^5\text{-}\eta^1\text{-}C_5H_4)_2Nb\text{-}\{(\mu\text{-}H)(\eta^5\text{-}C_5H_4B(C_6F_5)_2)\}][HB(C_6F_5)_3]$ (1) and $CpNb(C_6F_5)\{(\mu\text{-}H)(\eta^5\text{-}C_5H_4B(C_6F_5)_2\}$ (2)**

| | 1 | 2 |
|---|---|---|
| empirical formula | $C_{74}H_{45}B_2F_{25}Nb_3$ | $C_{28}H_{10}BF_{15}Nb$ |
| fw | 1709.45 | 735.08 |
| $T$, °C | −100 | −70 |
| cryst size (mm) | 0.19 × 0.17 × 0.15 | 0.38 × 0.35 × 0.35 |
| radiation ($\lambda$, Å) | MoKα (0.71073) | MoKα (0.71073) |
| cryst syst | monoclinic | orthorhombic |
| space group | *C*2/*c* | *Pbca* |
| $a$, Å | 19.536(1) | 15.536(1) |
| $b$, Å | 13.268(1) | 16.083(1) |
| $c$, Å | 51.378(1) | 19.639(1) |
| $\beta$, deg | 98.86(1) | |
| $V$, Å$^3$ | 13158(1) | 4907.2(5) |
| $Z$ | 8 | 8 |
| density (calcd, g/cm$^3$) | 1.726 | 1.990 |
| $\mu$, mm$^{-1}$ | 0.630 | 0.626 |
| 2$\theta$ range (deg) | 4.60 to 50.12 | 4.90 to 50.04 |
| no. of reflns collected | 40 509 | 20 429 |
| no. of ind reflns | 11 582 | 4339 |
| $R_{int}$ | 0.0919 | 0.0326 |
| max/min. transmn | 0.9114, 0.8896 | 0.8108, 0.7970 |
| no. of data/restraints/ params | 11582/0/962 | 4339/0/410 |
| goodness-of-fit on $F^2$ | 1.048 | 1.032 |
| final $R$ indices [$I = 2\sigma(I)$][a,b] | $R_1 = 0.0582$, $wR_2 = 0.1205$ | $R_1 = 0.0271$, $wR_2 = 0.0641$ |
| final $R$ indices (all data) | $R_1 = 0.1114$, $wR_2 = 0.1402$ | $R_1 = 0.0379$, $wR_2 = 0.0683$ |
| largest diff peak and hole (e Å$^{-3}$) | 0.633 and −0.720 | 0.319 and −0.329 |

[a] $R_1 = \sum||F_o| - |F_c||/\sum|F_o|$. [b] $wR_2 = \{\sum wF_o^2 - F_c^2)^2/\sum w(F_o^2)^2\}^{1/2}$.

metal−metal bond between them, Nb2 and Nb3 have coordination environments similar to Nb1: two $\eta^5$-coordinated Cp groups, a bridge hydrogen, and one $\eta^1$-$C_5H_4$ unit in which the Nb−C $\sigma$ bond distances (2.218(6)−2.294(6) Å) are in general slightly shorter than the Nb−C $\sigma$ bond distances in $[(\eta^5\text{-}C_5H_5)(\eta^5\text{-}\eta^1\text{-}C_5H_4)NbH]_2$ (2.297(3)−2.439(8) Å).[12] The distance of the $\sigma$ bond B1−C30 of the $BC_5H_4$ unit, 1.579(2) Å, is slightly shorter than that reported for B−C(aryl) bond distances (ca. 1.60 Å).[13] However, the B−C distances in the $BC_6F_5$ units of the cation are slightly longer (1.625(10)−1.629(11) Å) and in the anion they are significantly longer (1.635(9)−1.653(9) Å) than reported B−C(aryl) distances.[14] These longer distances are believed to reflect the electron-withdrawing effect of the pentafluorphenyl ring on the electron pair in the covalent B−C bond. The distances Nb−Centroid ($\eta^5$-$\eta^1$-Cp) (2.033−2.054 Å) are shorter than Nb−Centroid ($\eta^5$-Cp) distances (2.079, 2.084 Å), which is consistent with Guggenberger and Tebbe's observations of 2.034 Å for the Nb−Centroid ($\eta^5$-$\eta^1$-Cp) and 2.075 and 2.082 Å for the Nb−Centroid ($\eta^5$-Cp) distances. The $\sigma$ bonds Nb2−C31, Nb3−C29 associated with $\eta^1$-$C_5H_4$ and B1−C30 associated with $BC_5H_4$ constrain the $C_5H_4$ rings closer to the metal centers. Each of these bonds is tilted with respect to the plane of the $C_5$ ring with a tilt angle of ∼30°, with the exception of the angle, ∼24°, between the Nb1−C21 bond and the plane of the associated $C_5$ ring. The long distance between Nb1 and Nb2 in the Nb1−H−Nb2 bridge, 3.370 Å, accommodates the smaller tilt angle.

The cation of complex **1** is paramagnetic. It contains one unpaired electron, believed to be located on Nb1. The ESR spectrum consists of a well-resolved decet signal ($^{93}$Nb, $I = 9/2$) in $CH_2Cl_2$. The $^{11}$B NMR spectrum of complex **1** in $CD_2Cl_2$ consists of a doublet due to the $[HB(C_6F_5)_3]^-$ anion at −25.1 ppm $J(^{11}B-^1H) = 96$ Hz and a broad signal at −15.4 ppm that is assigned to the boron atom of the cation.

Boron-11 NMR spectra of reaction mixtures of $Cp_2Nb\{(\mu\text{-}H)_2BC_4H_8\}$ with $B(C_6F_5)_3$ in toluene were studied over the temperature range −70 to 27 °C. No reaction was indicated until the temperature reached −10 °C. Intermediate species formed could not be detected over the temperature range studied. Only the starting materials and the final products could be detected in the $^{11}$B NMR spectra.

**Formation of $CpNb(C_6F_5)\{(\mu\text{-}H)(\eta^5\text{-}C_5H_4B(C_6F_5)_2)\}$, 2, in the Coordinating Solvent Diethyl Ether.** In diethyl ether, the reaction between $Cp_2Nb\{(\mu\text{-}H)_2BR_2\}$ ($R_2 = C_4H_8$, $C_5H_{10}$, $C_8H_{14}$) and $B(C_6F_5)_3$ produces the molecular complex $CpNb(C_6F_5)\{(\mu\text{-}H)(\eta^5\text{-}C_5H_4B(C_6F_5)_2)\}$, **2** (reaction 2). $Nb^{III}$ is oxidized to $Nb^{IV}$ with the evolution

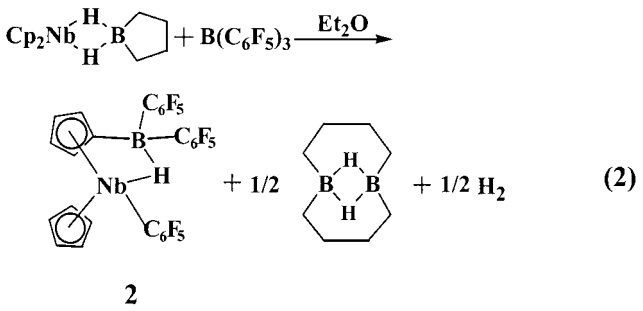


**2**

of $H_2$ in this reaction. The ESR spectrum in $CD_2Cl_2$ reveals a well-resolved decet. The other product depends on the cyclic organohydroborate ligand employed. The transannular hydrogen-bridged 10-membered cyclic organodiborane $B_2(\mu\text{-}H)_2(\mu\text{-}C_4H_8)_2$[10] is formed when $R_2 = C_4H_8$ (reaction 2), and the organodiboranes $(\mu\text{-}H)_2(BC_5H_{10})_2$[10] and $(\mu\text{-}H)_2(BC_8H_{14})_2$[10] are formed when $R_2 = C_5H_{10}$ and $C_8H_{14}$, respectively. Yields are in the range 70−75%. This compound is soluble in $CH_2Cl_2$. It is slightly soluble in diethyl ether, and it forms weak adducts in THF and pyridine. Solid **2** is green-brown in color. It is stable at room temperature in the absence of air.

The molecular structure of complex **2**, shown in Figure 3, was determined by single-crystal X-ray analysis. Crystal data are given in Table 1, and selected bond angles and distances are given in Table 3. A $C_5H_4$ ring is $\eta^5$-coordinated to Nb1 and $\eta^1$-coordinated to a $B(C_6F_5)_2$ group, while niobium and boron are linked through a Nb1−H−B bridge. A Cp ring and a $C_6F_5$ ring are also bound to Nb1 through $\eta^5$ and $\eta^1$ coordination, respectively. The bond Nb1−C111, with a distance of 2.282(2) Å, is significantly longer than all of the $\sigma$ Nb−C bond distances of the Nb($\eta^1$-$C_5H_4$) units in **1** (2.218(6), 2.223(6), and 2.229(6) Å). The $\sigma$ B1−C10 bond distance, 1.592(4) Å, in the B−$C_5H_4$ unit is comparable to that of the B1−C30 distance in **1**. The $\sigma$ B−C bond distances of the $BC_6F_5$ units, 1.621(4), 1.611(4) Å, are comparable to

(12) (a) Guggenberger, L. J.; Tebbe, F. N. *J. Am. Chem. Soc.* **1971**, *93*, 5924. (b) Guggenberger, L. J. *Inorg. Chem.* **1973**, *12*, 294.
(13) Allen, F. H.; Kennared, Watson, D. G.; Brammer, L.; Orpen, A. G.; Taylor, R. *J. Chem. Soc., Perkin Trans. 2* **1987**, S1.
(14) Otwinowski, Z.; Minor, W. In *Methods in Enzymology*; Carter, C. W., Jr., Sweet, R. M., Eds.; Academic Press: New York, 1997; Vol. 276(A), p 307.

**Table 2. Selected Bond Lengths (Å) and Angles (deg) for $[Cp_2Nb(\mu\text{-}H)(\eta^5\text{-}\eta^1\text{-}C_5H_4)Nb(\eta^5\text{-}\eta^1\text{-}C_5H_4)_2Nb\{(\mu\text{-}H)(\eta^5\text{-}C_5H_4B(C_6F_5)_2)\}][HB(C_6F_5)_3]$ (1)**

Bond Lengths

| | | | |
|---|---|---|---|
| Nb(1)−C(21) | 2.218(6) | Nb(3)−Centroid$_{(C36-C30)}$ | 2.047 |
| av Nb(1)−C(11−15) | 2.399 | Nb(3)−C(20) | 2.229(6) |
| av Nb(1)−C(16−10) | 2.388 | Nb(3)- - -B(1) | 2.712(8) |
| Nb(1)−Centroid$_{(C11-C15)}$ | 2.084 | Nb(3)−H(B) | 1.94(6) |
| Nb(1)−Centroid$_{(C16-C10)}$ | 2.079 | C(30)−B(1) | 1.579(11) |
| Nb(1)−HA | 1.86(9) | B(1)−C(111) | 1.625(10) |
| Nb(2)−C(31) | 2.223(6) | B(1)−C(121) | 1.629(11) |
| ave Nb(2)−C(21−25) | 2.382 | B(1)−H(B) | 1.32(7) |
| ave Nb(2)−C(26−20) | 2.370 | C(111)−C(116) | 1.374(10) |
| Nb(2)−Centroid$_{(C21-C25)}$ | 2.054 | C(111)−C(112) | 1.398(10) |
| Nb(2)−Centroid$_{(C26-C20)}$ | 2.040 | C(112)−F(112)[a] | 1.341(8) |
| Nb(2)−Nb(3) | 3.1208(8) | B(2)−C(211)[a] | 1.653(9) |
| Nb(2)−HA | 2.06(9) | B(2)−C(221)[a] | 1.635(9) |
| ave Nb(3)−C(31−35) | 2.365 | B(2)−C(231)[a] | 1.638(9) |
| ave Nb(3)−C(36−30) | 2.375 | B(2)−H(2)[a] | 1.07(5) |
| Nb(3)−Centroid$_{(C31-C35)}$ | 2.033 | | |

Bond Angles

| | | | |
|---|---|---|---|
| Centroid$_{(C11-C15)}$−Nb(1)−Centroid$_{(C16-C10)}$ | 134.3 | Centroid$_{(C31-C35)}$−Nb(3)−Nb(2) | 78.6 |
| Centroid$_{(C11-C15)}$−Nb(1)− C(21) | 108.7 | Centroid$_{(C36-C30)}$−Nb(3)−Nb(2) | 120.1 |
| Centroid$_{(C16-C10)}$−Nb(1)− C(21) | 110.8 | Centroid$_{(C31-C35)}$−Nb(3)−H(B) | 104.6 |
| Centroid$_{(C11-C15)}$−Nb(1)−H(A) | 106.9 | Centroid$_{(C36-C30)}$−Nb(3)−H(B) | 94.3 |
| Centroid$_{(C16-C10)}$−Nb(1)−H(A) | 104.2 | C(20)−Nb(3)−H(B) | 83(2) |
| C(21)−Nb(1)−H(A) | 77(3) | C(39)−C(30)−B(1) | 124.7(7) |
| Centroid$_{(C21-C25)}$−Nb(2)−Centroid$_{(C26-C20)}$ | 136.3 | C(36)−C(30)−B(1) | 118.8(6) |
| Centroid$_{(C21-C25)}$−Nb(2)−C(31) | 110.6 | C(30)−B(1)−C(111) | 118.1(6) |
| Centroid$_{(C26-C20)}$−Nb(2)−C(31) | 108.9 | C(30)−B(1)−C(121) | 113.1(7) |
| Centroid$_{(C21-C25)}$−Nb(2)−H(A) | 101.8 | C(111)−B(1)−C(121) | 113.1(6) |
| Centroid$_{(C26-C20)}$−Nb(2)−H(A) | 100.7 | C(30)−B(1)−H(B) | 99(3) |
| Centroid$_{(C21-C25)}$−Nb(2)−Nb(3) | 117.1 | C(111)−B(1)−H(B) | 102(3) |
| Centroid$_{(C26-C20)}$−Nb(2)−Nb(3) | 78.4 | C(121)−B(1)−H(B) | 109(3) |
| C(31)−Nb(2)−H(A) | 83(2) | C(116)−C(111)−C(112) | 113.9(7) |
| C(31)−Nb(2)−Nb(3) | 47.0(2) | C(116)−C(111)−B(1) | 124.2(7) |
| Centroid$_{(C31-C35)}$−Nb(3)−Centroid$_{(C36-C30)}$ | 137.6 | C(112)−C(111)−B(1) | 121.8(6) |
| Centroid$_{(C31-C35)}$−Nb(3)−C(20) | 109.3 | F(112)−C(112)−C(113) | 118.0(8) |
| Centroid$_{(C36-C30)}$−Nb(3)−C(20) | 110.4 | F(112)−C(112)−C(111) | 119.3(6) |

[a] Bond lengths in the$[HB(C_6F_5)_3]^-$ anion.



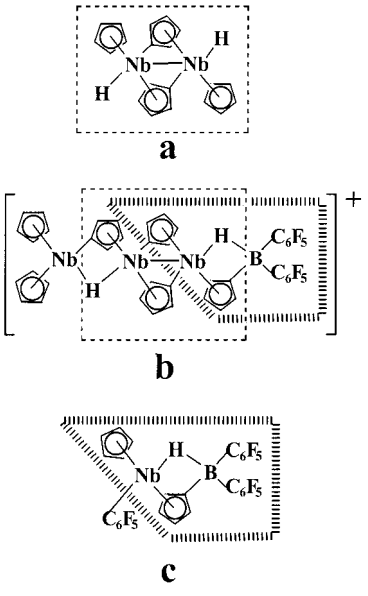


**Figure 2.** Comparison of structural features of complex **1** (b) with those of $[(\eta^5\text{-}C_5H_5)(\eta^5\text{-}\eta^1\text{-}C_5H_4)NbH]_2$ (a) and those of complex **2** (c).

those in **1**. Because of the constraints imposed by Nb1−H1−B1 and B1−C10 of the $C_5H_4$ unit, the NB1−Centroid(C16−C10) distance, 2.038 Å, is shorter than the Nb1−Centroid(C11−C15) distance, 2.072 Å, which results in the B1−C10 bond being bent ∼30° out of the $C_5H_4$ plane.

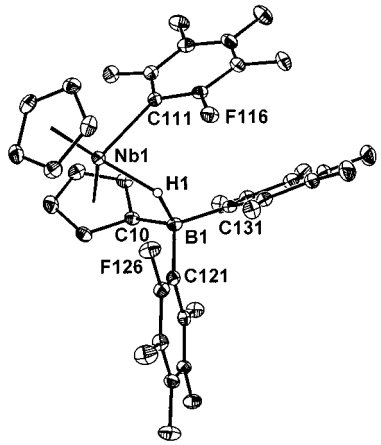


**Figure 3.** Molecular structure of $CpNb(C_6F_5)\{(\mu\text{-}H)(\eta^5\text{-}C_5H_4B(C_6F_5)_2)\}$, **2**.

The $^{11}B$ NMR spectrum of complex **2** in $CD_2Cl_2$ consists of a sharp resonance at −15.4 ppm, which is similar to the $^{11}B$ signal of the cation in **1**. The bridge hydrogen could not be detected in the $^1H$ NMR spectrum.

In THF, complex **2** forms a weak adduct through addition of the THF to niobium with cleavage of the Nb−H−B hydrogen bridge bond at the Nb−H site. The resulting bridge cleavage product contains a terminal B−H bond, as indicated by a doublet in the $^{11}B$ NMR spectrum ($\delta = -24.9$ ppm; $J(d,^{11}B-^1H) = 89$ Hz). This adduct, $(CpNb(C_6F_5)(THF)\{\eta^5\text{-}C_5H_4B(H)(C_6F_5)_2\}$, is zwitterionic. It is represented in reaction 3 as an **A** type

**Table 3. Selected Bond Lengths (Å) and Angles (deg) for $CpNb(C_6F_5)\{(\mu\text{-}H)(\eta^5\text{-}C_5H_4B(C_6F_5)_2)\}$ (2)**

| | | | |
|---|---|---|---|
| **Bond Lengths** | | | |
| Nb(1)−C(111) | 2.282(2) | B(1)−H(1) | 1.32(2) |
| av Nb(1)−C(11−15) | 2.390 | C(121)−C(126) | 1.378(3) |
| av Nb(1)−C(16−10) | 2.366 | C(121)−C(122) | 1.384(3) |
| Nb(1)−Centroid$_{(C11-C15)}$ | 2.072 | C(122)−F(122) | 1.354(3) |
| Nb(2)−Centroid$_{(C16-C10)}$ | 2.038 | C(111)−C(112) | 1.384(3) |
| Nb(1)- - -B(1) | 2.742(3) | C(112)−F(112) | 1.360(3) |
| Nb(1)−H(1) | 1.94(2) | B(1)−C(121) | 1.621(4) |
| C(10)−B(1) | 1.592(4) | B(1)−C(131) | 1.611(4) |
| **Bond Angles** | | | |
| Centroid$_{(C11-C15)}$−Nb(1)−Centroid$_{(C16-C10)}$ | 40.3 | C(131)−B(1)−H(1) | 104(1) |
| Centroid$_{(C11-C15)}$−Nb(1)−C(111) | 106.3 | C(10)−B(1)−C(121) | 112.9(2) |
| Centroid$_{(C16-C10)}$−Nb(1)−C(111) | 107.8 | C(131)−B(1)−C(121) | 112.0(2) |
| Centroid$_{(C11-C15)}$−Nb(1)−H(1) | 112.3 | C(132)−C(131)−B(1) | 127.1(2) |
| Centroid$_{(C16-C10)}$−Nb(1)−H(1) | 92.0 | C(136)−C(131)−B(1) | 119.0(2) |
| C(10)−B(1)−C(131) | 123.1(2) | F(132)−C(132)−C(133) | 116.6(2) |
| C(121)−B(1)−H(1) | 105(1) | F(132)−C(132)−C(131) | 120.4(2) |
| C(111)−Nb(1)−H(1) | 82.7(7) | C(133)−C(132)−C(131) | 123.0(2) |
| C(10)−B(1)−H(1) | 97(1) | C(112)−C(111)−Nb(1) | 124.6(2) |
| C(116)−C(111)−C(112) | 113.1(2) | C(16)−C(17)−Nb(1) | 70.5(1) |
| C(116)−C(111)−Nb(1) | 122.0(2) | C(18)−C(17)−Nb(1) | 72.7(2) |
| F(112)−C(112)−C(111) | 119.8(2) | C(16)−C(17)−H(17) | 126.1 |
| F(112)−C(112)−C(113) | 116.0(2) | C(16)−C(10)−C(19) | 105.1(2) |
| C(111)−C(112)−C(113) | 124.2(2) | C(16)−C(10)−B(1) | 127.3(2) |
| C(16)−C(17)−C(18) | 107.8(2) | C(19)−C(10)−B(1) | 117.3(2) |



cleavage product. Complex **2** also forms weak adducts

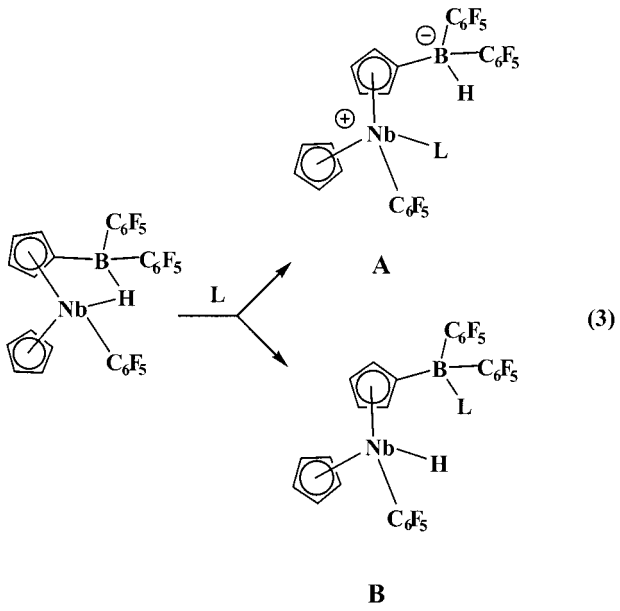


with pyridine. In pyridine, the predominant adduct of **2** is $CpNb(C_6F_5)(Py)\{\eta^5\text{-}C_5H_4B(H)(C_6F_5)_2\}$, also of the **A** type, producing a $^{11}B$ NMR spectrum of a well-resolved doublet ($\delta$ −24.9 $J(^{11}B-^{1}H) = 90$ Hz). To a lesser extent, an additional product is observed in the $^{11}B$ NMR spectrum. This product produces a broad $^{11}B$ NMR singlet ($\delta = -4.4$ ppm) that is assigned to a B−N bond. This suggests that this complex is formed through cleavage of the Nb−H−B bond at the H−B site to yield the complex $CpNb(C_6F_5)(H)\{\eta^5\text{-}C_5H_4B(Py)(C_6F_5)_2\}$, represented in reaction 3 as compound **B**. The THF and pyridine adducts of complex **2** could not be isolated. They dissociate upon pumping to dryness the THF and pyridine solutions to yield solid **2**.

The $^{11}B$ NMR spectra of the reaction mixture of $Cp_2Nb\{(\mu\text{-}H)_2BC_4H_8\}$ with $B(C_6F_5)_3$ in diethyl ether were studied over the temperature range −70 to 27 °C. The reaction proceeds slowly at −70 °C. Starting materials $Cp_2Nb\{(\mu\text{-}H)_2BC_4H_8\}$ ($\delta$ = 61.4 ppm), $Et_2OB(C_6F_5)_3$ ($\delta$ = 3.8 ppm), and an intermediate species with a very sharp signal at −15.2 ppm are observed. A weaker signal, a poorly resolved doublet, is seen at −24.9 ppm. This signal is consistent with the formation of a diethyl ether adduct, $CpNb(C_6F_5)(Et_2O)\{\eta^5\text{-}C_5H_4B(H)(C_6F_5)_2$, like the THF and pyridine adducts of **A** type represented by reaction 3. The very sharp signal at −15.2 ppm (19 Hz at half-height) is close to that of **2** (−15.4 ppm) but is believed to be due to an intermediate species since **2** is insoluble in diethyl ether and its signal is broader (43 Hz at half-height in $CD_2Cl_2$). The signal for the intermediate product shifts to lower field with higher temperature, −14.4 ppm. Above 20 °C, the reaction proceeds sufficiently rapidly that the intermediate is no longer detectable, but the signal assigned to the diethyl ether adduct of **2** is the predominant one. Upon standing at room temperature, complex **2** slowly precipitates from the solution. Cooling the solution to −90 °C in 10 °C increments did not cause the reappearance of the signal assigned to the intermediate species.

## Summary and Discussion

Results from the present work (summarized in reactions 1 and 2) are in sharp contrast with those from the reactions of the related complexes $Cp_2Ti\{(\mu\text{-}H)_2BR_2\}$ ($R_2 = C_4H_8$, $C_5H_{10}$, $C_8H_{14}$)[8] with $B(C_6F_5)_3$ (summarized in Scheme 1, **c** and **d**). The only differences between these complexes are the atomic number of Ti and Nb and the ease of oxidation from the III to the IV state. It is of interest to summarize the differences in results. In the poorly coordinating solvent toluene, $Cp_2Ti\{(\mu\text{-}H)_2B(C_6F_5)_2\}$ is produced, but in the coordinating solvent diethyl ether, $[Cp_2Ti(OEt_2)_2]^?[HB(C_6F_5)_3]^-$ is produced. On the other hand $Cp_2Nb\{(\mu\text{-}H)_2BR_2\}$ ($R_2 = C_4H_8$, $C_5H_{10}$, $C_8H_{14}$) produces $[Cp_2Nb(\mu\text{-}H)(\eta^5\text{-}\eta^1\text{-}C_5H_4)Nb(\eta^5\text{-}\eta^1\text{-}C_5H_4)_2Nb\{(\mu\text{-}H)(\eta^5\text{-}C_5H_4B(C_6F_5)_2)\}]^+[HB$-

$(C_6F_5)_3]^-$, **1**, in toluene and $CpNb(C_6F_5)\{(\mu\text{-}H)(\eta^5\text{-}C_5H_4B(C_6F_5)_2)\}$, **2**, in diethyl ether. Furthermore, while the oxidation state of $Ti^{III}$ is unchanged in its reactions, niobium is oxidized from $Nb^{III}$ to $Nb^{IV}$.

Some structural features of the triniobocene cation of complex **1** and the covalent complex **2** are in common with the covalent, diamagnetic, $Nb^{IV}$ complex $[(\eta^5\text{-}C_5H_5)(\eta^5\text{-}\eta^1\text{-}C_5H_4)NbH]_2$[12] (Figure 2a) and with each other (Figure 2, b and c). In general, distances and angles involving corresponding atoms are in accord with those reported for $[(\eta^5\text{-}C_5H_5)(\eta^5\text{-}\eta^1\text{-}C_5H_4)NbH]_2$.[12]

The reactions by which compounds **1** and **2** are formed do not lend themselves to the isolation and or identification of intermediate species. In the case of compound **1**, the presence of intermediate species could not be detected. Although $^{11}B$ NMR spectroscopy did indicate the presence of a low-temperature intermediate in the formation of compound **2**, isolation and identification of the intermediate was not achieved. However, it is possible to comment on the formation of the covalent complex **2** in that it appears that its immediate precursor is the **A** type zwitterionic complex $CpNb(C_6F_5)(Et_2O)\{\eta^5\text{-}C_5H_4B(H)(C_6F_5)_2\}$. At room temperature complex **2** slowly precipitates from solution. Presumably diethyl ether is slowly eliminated from the type **A** complex, resulting in the formation and precipitation of **2**.

## Experimental Section

**General Procedures.** All manipulations were carried out on a standard high-vacuum line or in a drybox under an atmosphere of nitrogen. Diethyl ether, THF, toluene, and pyridine were dried over sodium benzophenone and freshly distilled prior to use. Methylene chloride was dried over $CaH_2$ and distilled before use. Reactions were carried out in the dry solvents under nitrogen. $B(C_6F_5)_3$ (Aldrich) was used as received. The complexes $Cp_2Nb\{(\mu\text{-}H)_2BR_2\}$ ($R_2 = C_4H_8$, $C_5H_{10}$, $C_8H_{14}$) were prepared by procedures described in the literature.[9] Elemental analyses were performed by Galbraith Laboratories, Knoxville, TN. Proton NMR spectra ($\delta$(TMS) 0.00 ppm) were recorded on a Bruker AM-250 NMR spectrometer operating at 250.11 MHz and on a Bruker AM-400 NMR spectrometer operating at 400.13 MHz. $^{11}B$ spectra (externally referenced to $BF_3{\cdot}OEt_2$ ($\delta$0 ppm)) were collected at 128.38 or 80.25 MHz as noted. Infrared spectra were recorded on a Mattson Polaris Fourier transform spectrometer with 2 $cm^{-1}$ resolution. ESR spectra for complexes **1** and **2** were observed at 25 °C in $CH_2Cl_2$ on a Bruker ESP300 ESR spectrometer at 9.75 GHz and 1.0 mW power. Both complexes produce similar well-resolved 10-line spectra, as expected for $d^1$, $^{93}Nb$ ($I = 9/2$) with the centers of the fields at 3515 G, $a = 115$ G and $g = 1.98$.

**X-ray Structure Determination.** Single-crystal X-ray diffraction data for **1** and **2** were collected on a Nonius KappaCCD diffraction system which employs graphite-monochromated Mo K$\alpha$ radiation ($\lambda = 0.71073$ Å). A single crystal was mounted on the tip of a glass fiber coated with Fomblin oil (a perfluoropolyether). Crystallographic data were collected at −100 °C for **1** and −70 °C for **2**. Unit cell parameters were obtained by indexing the peaks in the first 10 frames and refined employing the whole data set. All frames were integrated and corrected for Lorentz and polarization effects using the Denzo-SMN package (Nonius BV, 1999).[14] Absorption correction was applied using the SORTAV program[15] provided by MaXus software.[16] The structures were solved by direct methods and refined using the SHELXTL-97 (difference electron density calculation, full matrix least-squares refinements) structure solution package.[17] Data merging was performed using the data preparation program supplied by SHELXTL-97. After all non-hydrogen atoms were located and refined anisotropically, H atoms of Cp rings were calculated assuming standard −CH geometries. All other hydrogen atoms were located and refined isotropically.

**Preparation of $[Cp_2Nb(\mu\text{-}H)(\eta^5\text{-}\eta^1\text{-}C_5H_4)Nb(\eta^5\text{-}\eta^1\text{-}C_5H_4)_2\text{-}Nb\{(\mu\text{-}H)(\eta^5\text{-}C_5H_4B(C_6F_5)_2)\}]^+[HB(C_6F_5)_3]^-$, 1.** Complex **1** was prepared from reactions of $Cp_2Nb\{(\mu\text{-}H)_2BC_4H_8\}$, $Cp_2Nb\{(\mu\text{-}H)_2BC_5H_{10}\}$, and $Cp_2Nb\{(\mu\text{-}H)_2BC_8H_{14}\}$ with $B(C_6F_5)_3$ in toluene under similar conditions and produced products in comparable yields. A typical synthetic procedure is described. In a drybox a 129 mg (0.42 mmol) quantity of $Cp_2Nb\{(\mu\text{-}H)_2BC_4H_8\}$ and 144 mg (0.28 mmol) of $B(C_6F_5)_3$ were put in a flask. After degassing, about 10 mL of toluene was transferred to the flask at −78 °C under vacuum. The system was warmed to room temperature. After stirring for 24 h, the brown-green solution was filtered and concentrated. During the reaction $H_2$ evolved and, in addition to complex **1**, the products $C_6F_5H$ (identified by GC−MS(EI): calcd for $C_6HF_5$, $m/z = 168.1$; obsd, $m/z = 168.1$) and $B_2(\mu\text{-}H)_2(\mu\text{-}C_4H_8)_2$ (identified by its $^{11}B$ NMR spectrum[10]) were generated. Crystallization of the solution at −18 °C produced brown crystals (116 mg, 48%), which were suitable for X-ray analysis. $^{11}B$ NMR (250 MHz, $CD_2Cl_2$, 25 °C): $\delta$ −25.1 (d, $J(^{11}B-^1H) = 96$ Hz, $[HB(C_6F_5)_3]^-$), −15.4 (s, $(\mu\text{-}H)(\eta^5\text{-}C_5H_4B(C_6F_5)_2)$. IR (KBr): 3124w, 2953m, 2924s, 2853s, 2360w, 1749w, 1646s, 1516s, 1477vs, 1443s, 1412s, 1384s, 1341m, 1290s, 1195w, 1100s, 1045m, 1011m, 974s, 893m, 826s, 794m, 762m, 729m, 680m, 632w, 606w, 576w, 567w, 542w, 505w. Anal. Calcd for $C_{74}H_{45}B_2F_{25}Nb_3$: C, 47.25; H, 1.92. Found: C, 46.99; H, 1.94.

**Preparation of $CpNb(C_6F_5)\{(\mu\text{-}H)(\eta^5\text{-}C_5H_4B(C_6F_5)_2)\}$, 2.** Complex **2** was prepared from reactions of $Cp_2Nb\{(\mu\text{-}H)_2BC_4H_8\}$, $Cp_2Nb\{(\mu\text{-}H)_2BC_5H_{10}\}$, and $Cp_2Nb\{(\mu\text{-}H)_2BC_8H_{14}\}$ with $B(C_6F_5)_3$ in diethyl ether under similar conditions and produced products in comparable yields. A typical synthetic procedure is described. In a drybox a 207 mg (0.71 mol) quantity of $Cp_2Nb\{(\mu\text{-}H)_2BC_4H_8\}$ and 363 mg (0.71 mmol) of $B(C_6F_5)_3$ were put in a flask. The flask was evacuated, and about 5 mL of diethyl ether was condensed into the flask at −78 °C. The system was warmed to room temperature. After stirring for 48 h, the brown-green solution was filtered and concentrated. During the reaction $H_2$ evolved, and in addition to complex **2**, the product $B_2(\mu\text{-}H)_2(\mu\text{-}C_4H_8)_2$ (identified by its $^{11}B$ NMR spectrum[10]) formed. Brown crystals for X-ray and chemical analysis were obtained at room temperature and washed with hexane (381 mg, 73%). To minimize contamination by unreacted $B(C_6F_5)_3$, toluene is a better agent for washing **2** free of contaminants. $^{11}B$ NMR (250 MHz, $CD_2Cl_2$, 25 °C): $\delta$ −15.4 (s, 43 Hz at half-height). IR (KBr): 3125s, 2977m, 2928m 2872m, 2603w, 2362m, 2090w, 1847w, 1646s, 1600m, 1520vs, 1455vs, 1382s, 1357s, 1290s, 1270s, 1255m, 1214m, 1187m, 1100s, 1060s, 1011s, 972s, 846s, 827s, 793s, 767s, 745m, 730m, 695m, 617w, 576w, 542m. Anal. Calcd for $C_{28}H_{10}BF_{15}Nb$: C, 45.75; H, 1.37. Found: C, 46.37; H, 1.16.

**Bridge Hydride Cleavage Reactivity of Compound 2.** Reaction of complex **2** with THF: A 34 mg sample of complex **2** was placed in 0.4 mL of $d_8$-THF in a quartz NMR tube that was then sealed. $^{11}B$ NMR (128.38 MHz, $d_8$-THF): $\delta$ −25.6, (d, $J(^{11}B-^1H) = 90$ Hz (d, $\eta^5\text{-}C_5H_4B(H)(C_6F_5)_2^-$). Reaction of complex **2** with pyridine: A 32 mg sample of complex **2** was

(15) (a) Blessing, R. H. *Acta Crystallogr., Sect. A* **1995**, *51*, 33. (b) Blessing, R. H. *J. Appl. Crystallogr.* **1997**, *30*, 421−426.

(16) Mackay, S.; Gilmore, C. J.; Edwards, C.; Tremayne, M.; Stuart, N.; Shankland, K. *MaXus: A computer program for the solution and refinement of crystal structures from diffraction data*; University of Glasgow: Scotland, Nonius BV: Delft, The Netherlands, and MacScience Co. Ltd.: Yokohama, Japan, 1998.

(17) Sheldrick, G. M. *SHELXTL-97: A Structure Solution and Refinement Program*; University of Göttingen: Germany, 1998.

placed in 0.4 mL of $d_5$-pyridine in a quartz NMR tube that was then sealed. $^{11}$B NMR (128.38 MHz, $d_5$-pyridine): $\delta$ −4.4 (br, $\eta^5$-$C_5H_4B$(Py)$(C_6F_5)_2$), −25.1(d, $J(^{11}B-^{1}H)$ = 90 Hz, $\eta^5$-$C_5H_4B(H)(C_6F_5)_2^-$).

The NMR tubes were opened under vacuum, and solvent was pumped away to dryness from pyridine and THF solutions. The remaining solids were dissolved in $CD_2Cl_2$. The $^{11}$B NMR spectra of the solution were that of complex **2**.

**Low-Temperature $^{11}$B NMR Study of Reaction Solutions.** Samples of $Cp_2Nb\{(\mu\text{-}H)_2BC_4H_8\}$ (20 mg, 0.067 mmol) and 23 mg(0.045 mmol) of $B(C_6F_5)_3$ (in 3:2 ratio) were placed in a quartz NMR tube with a graded seal. The tube was evacuated, and about 0.4 mL of toluene was condensed into the tube at −78 °C and was then sealed. Boron-11 NMR spectra were taken at every 10 °C starting from −70 to 27 °C at 128.38 MHz. From −70 to −20 °C the signals observed were −3.4 ppm ($B(C_6F_5)_3$) and 59.2 ppm ($Cp_2Nb\{(\mu\text{-}H)_2BC_4H_8\}$). The reaction proceeds slowly above −10 °C. As the temperature is raised, new signals appear at 29.0 ppm (br, $B_2(\mu\text{-}H)_2(\mu\text{-}C_4H_8)_2$) and −24.8 ppm (d, $J(^{11}B-^{1}H)$ = 90 Hz, $[HB(C_6F_5)_3]^-$). There is no indication of the formation of an intermediate species formed over the temperature range studied.

Samples of $Cp_2Nb\{(\mu\text{-}H)_2BC_4H_8\}$ (23 mg, 0.075 mmol) and 38 mg (0.074 mmol) of $B(C_6F_5)_3$ (in 1:1 ratio) were placed in a quartz NMR tube with a graded seal. The tube was evacuated, and about 0.4 mL of diethyl ether was condensed into the tube at −78 °C which was then sealed. The Boron-11 NMR spectra were taken at every 10 °C interval starting from −70 to 27 °C and from 27 to −90 °C at 128.38 MHz. The reaction proceeds slowly at −70 °C. Signals appear at 61.4 ppm (br, $Cp_2Nb(\mu\text{-}H)_2BC_4H_8$), 3.8 ppm (br, $Et_2OB(C_6F_5)_3$), and −15.2 ppm (very sharp, width at half-height = 19 Hz, unidentified), ca. −24.9 ppm (br, very weak, $CpNb(C_6F_5)(Et_2O)\{\eta^5\text{-}C_5H_4B(H)(C_6F_5)_2\}$). With an increase in temperature the signals at −15.2 and −24.9 ppm move to slightly lower field. At 10 °C these signals shift to −14.4 and −23.9 ppm, respectively, and a new signal at 29.0 ppm (br, $B_2(\mu\text{-}H)_2(\mu\text{-}C_4H_8)_2$) appears. Above 20 °C, the reaction proceeds sufficiently rapidly that the signal at −14.4 ppm is no longer detectable, but the signal at −23.9 ppm is the predominant signal. Upon standing at room temperature, complex **2** slowly precipitates from the solution. The unit cell and space group of this crystalline precipitate are in excellent agreement with those parameters of **2**. Cooling the solution to −90 °C produces no evidence for the emergence of the signal attributed to the intermediate product which appeared at low temperature when the reaction was initiated.

**Acknowledgment.** This work was supported by the National Science Foundation through Grants CHE 97-00394 and CHE 99-01115. We thank Dr. Johnie Brown of the Campus Chemical Instrument Center for obtaining the GC−MS spectra.

**Supporting Information Available:** Molecular structure of compound **1**; molecular structure of compound **2**; tables of crystallographic data, positional and thermal parameters, and interatomic distances and angles for **1**, **2**; ESR spectra of compound **1** and **2**. Two X-ray crystallographic files in CIF format. This material is available free of charge via the Internet at http://pubs.acs.org.

OM0107744